DOI:10.1021/jf901593m

JOURNAL OF AGRICULTURAL AND FOOD CHEMISTRY
ARTICLE

# Starch Granules in Tomato Fruit Show a Complex Pattern of Degradation

KIETSUDA LUENGWILAI AND DIANE M. BECKLES*

Department of Plant Sciences MS-3, University of California, One Shields Avenue, Davis, California 95616

Starch is transiently accumulated in tomato fruit with near complete degradation achieved by maturity. Surprisingly, $^{14}$C-pulse-chase analyses indicated that the rate of starch degradation was highest in immature fruit [10 days post anthesis (DPA)] when maximal synthesis occurs, but was almost undetectable at 45 DPA when there is net breakdown of starch. Further analysis of starch accumulation, rate of synthesis, particle size analysis, and confocal laser scanning microscopy of starch granules from developing fruit suggests that the rate of starch degradation does increase after 40 DPA, but it may not occur at the same site at which starch is synthesized. Furthermore, the degradation rate at maturity is lower than that measured in early development. Overall, the results suggest that starch degradation in developing tomato is biphasic with separate regiotemporal occurrences. This mechanism may have evolved to offer flexibility in balancing starch accumulation and utilization in the developing fruit.

**KEYWORDS: Tomato starch; starch granule; starch degradation; $^{14}$C-glucose labeling**

## INTRODUCTION

Tomato is an important horticultural crop with global production reaching 126 M tonnes pa in 2007 and with U.S. farm gate values of $2 billion (*1*). The rate at which starch accumulates correlates positively with fruit growth, and manipulating starch has been regarded as a good approach for tomato improvement (*2*). Starch is transiently accumulated in tomato fruit and is both synthesized and degraded over ~49 days (*3*, *4*). This pattern is similar to that in oilseeds (*5*) but contrasts with well-studied systems such as in leaves, where synthesis and degradation occur within 24 h of synthesis, and tubers and cereal endosperm, where these processes are intergenerational (*6*). The distinct spatiotemporal occurrence of starch degradation between species suggests that each may have unique pathways for this process (*6*).

Another important feature of starch metabolism in fruit and oilseeds is that starch may be degraded during active synthesis (*6*). Enzymes capable of degrading starch have been detected in the plastids of young oilseeds and tomato fruit (*5*, *7*−*9*), and the amount of plastid amylolytic activity was similar to that of starch biosynthetic enzymes (*9*). In addition, tomato fruit can synthesize starch during the period of net starch breakdown, illustrating that these two mechanisms can coexist (*10*, *11*). These lines of evidence suggest that starch turnover occurs in these organs but do not provide direct proof thereof. N'tchobo et al. proposed that starch turnover occurs at all stages of tomato fruit development on the basis of pulse-chase experiments, but the data were not clear (*10*). They showed increased incorporation of radiolabel into starch during the chase, which is the opposite of that expected if turnover was occurring. Interestingly, unambiguous evidence that starch turnover occurs during net accumulation in major starch-storage organs has not been shown. For example, the cases of turnover cited in ref *12* were tissues (i) that are not primary starch storers, for example, *Ricinus* seedlings and spinach chloroplasts; (ii) that were undergoing senescence, that is, fruit ripened postharvest; or (iii) that were genetically engineered.

The way in which the tomato starch granule is attacked during degradation is also unknown. This may be of commercial interest because granule breakdown may influence sugar availability in fruit. Furthermore, if the granule is degraded during active synthesis, tomato fruit may offer new insight into this process. We showed previously that starch granules increase in size throughout fruit development, even in ripening (*13*), suggesting that, as in cereals, digestion occurs from the inside-out (*14*); however, this would need to be tested directly to rule out other mechanisms that may also exist. On the basis of various descriptions in the literature there are potentially four primary ways in which tomato starch granules may be degraded in vivo (see **Figure 1**). The first model, A, is based on "centrifugal digestion" or breakdown of starch in the center of the granule. The second model, B, "centripetal digestion", is based on attack of the granule at the surface. The third model, C, assumes centripetal digestion and granule aggregation. The fourth model, D, is based on the continued synthesis of starch during ripening in combination with centrifugal digestion (*13*). The events depicted in each model are not mutually exclusive, and all of these processes could be occurring to various degrees.

The aim of this study therefore was to examine starch granule degradation and synthesis in developing tomato fruit. The specific questions we asked were the following: (1) Are the starch granules in tomato fruit degraded during the phase of net starch accumulation? (2) How are the starch granules from tomato fruit degraded? We designed several experiments to address these questions and to identify which model of starch granule metabolism best describes

 Published on Web 08/24/2009 

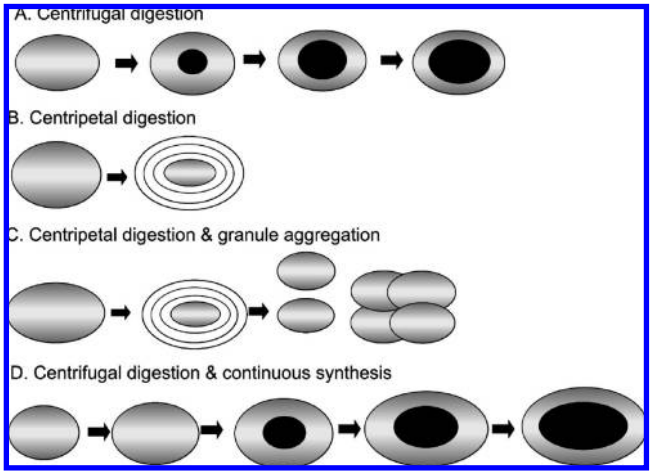


**Figure 1.** Four models of starch digestion in ripening tomato fruit based on published data (*6*, *13*): (**A**) centrifugal digestion (assumes minimal accumulation at the surface with loss of internal glucan initiated at the core; found in cereal endosperm and in starch granules digested in vitro with amylases); (**B**) centripetal digestion (loss of glucan is primarily at the granule surface; occurs in *Arabidopsis* leaves, potato tuber, and canna rhizome starches); (**C**) centripetal digestion and granule aggregation [based on observations that granule size increases from young (16 DPA) to mature green, during which time starch degradation occurs and plastids in ripening tomato fruit fuse]; (**D**) centrifugal digestion with granule growth by continued deposition of starch at the surface.

that occurring in vivo. Collectively, our findings could broaden our understanding of the mechanisms governing starch degradation in tomato fruit.

## MATERIALS AND METHODS

**Purification and in Vitro Digestion of Starch.** Starch granules from pericarp and columella of developing tomato fruit were purified as described previously except that these fractions were mixed (*13*). Starch from three individual fruits at each stage was extracted separately, and all results are the mean ± SEM of these three biological replicates unless otherwise stated. Aliquots of 150 mg of starch from mature green fruit were digested with α-amylase isolated from *Aspergillus niger* (Sigma-Aldrich, St. Louis, MO) at a final concentration of 100 U $mg^{-1}$ starch in a 15 mL volume of sodium acetate, pH 4.8, at 37 °C. Aliquots of the suspension (2 mL) were removed after 0, 3, 6, 12, 24, 54, and 72 h; the samples were spun at 15000 *g* for 10 min, and the pellet was washed three times in 80% (v/v) ethanol and then twice in 100% (v/v) acetone. The powder was allowed to dry by evaporation of acetone. The supernatant was saved for measurements of glucose using the Glucose (HK) Assay (GAHK-20) kit from Sigma-Aldrich.

**Scanning Electron Microscopy (SEM) and Starch Particle Size Distribution.** This was done as described by Luengwilai and Beckles (*13*).

**Starch and Glucose Measurements.** Starch and sugars were determined using the method outlined previously (*7*) after samples had been boiled in 80% (v/v) ethanol. Starch was assayed as the glucose released after enzymatic digestion of the ethanol-insoluble fraction using the Glucose HK Assay Kit from Sigma (St. Louis, MO).

**Confocal Laser Scanning Microscopy (CLSM).** Starch granules were mixed into a solution of *d*-limonene containing 0.1 mg $mL^{-1}$ Nile Red for 1 h (*15*). A confocal laser scanning microscope (CLSM) Fluoview FV1000 (Olympus Optical Co. America Inc.) with a He−Ne laser was used to visualize the Nile Red within the starch granules. The microscope was set on an emission wavelength of 544 nm, and emission of Nile Red was at 628 nm. All confocal fluorescence images were taken with a 60× objective. The software used for CLSM imaging was Olympus Fluoview FV10-ASW software (version 1.4a; Olympus Corp.).

**Radiolabeling of Starch with [U-$^{14}$C]Glucose.** Tomato fruits were sampled at different stages and incubated with radiolabel as described by

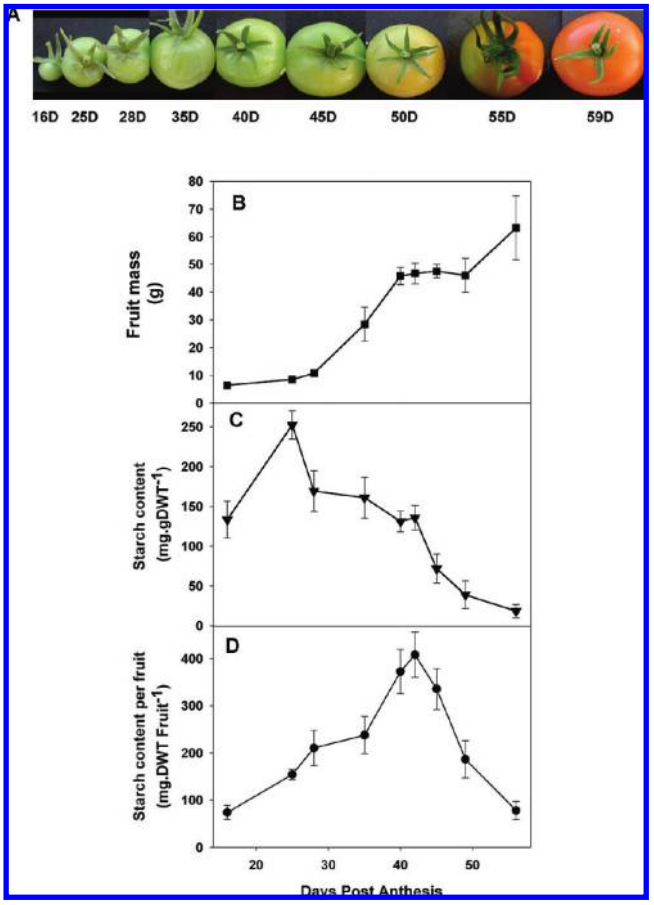


**Figure 2.** Changes in phenotype, fresh weight, and starch content of developing tomato fruit: (**A**) tomato fruit sampled at different developmental stages as indicated; (**B**) fruit fresh weight; (**C**) starch content $gDWT^{-1}$; (**D**) starch content $gDWT^{-1}$ $fruit^{-1}$. Values are the mean ± SE of three to six fruit.

Carrari et al. (*11*). Briefly, disks (10 mm in diameter, 1.5 mm thick) were excised from fruit with a cork borer, and the epidermis was removed. The disks were washed three times in 10 mM 2-[*N*-morpholino]ethanesulfonic acid] (MES)−KOH, pH 6.8, and then incubated in [U-$^{14}$C]glucose (Sigma) of specific activity 1.4 MBq $mmol^{-1}$ with 10 mM glucose for 2 h at 25 °C. After incubation, the disks were washed three times in 10 mM MES−KOH with 10 mM glucose and then snap-frozen in liquid nitrogen. Total radioactivity incorporated was determined by liquid scintillation counting after fractionation of the labeled tissue. The homogenized tissues were boiled four times for 5 min in 80% (v/v) ethanol and the soluble and insoluble fractions separated. The insoluble fraction was then boiled for 1 h to gelatinize starch; then three 200 μL aliquots of the insoluble fraction were digested with amyloglucosidase at 10 U per 200 μL (Roche; Nutley, NJ), and the $^{14}$C in the resulting supernatant was counted. For the pulse-chase experiment 8 mm disks were sampled from the pericarp of three to five fruits and incubated in [U-$^{14}$C]glucose of specific activity 2.8 MBq $mmol^{-1}$ supplemented with 10 mM glucose for 30 min. The disks were washed three times followed by chase periods of 1.3, 2.7, and 4 h in 10 mM MES with 10 mM glucose. After incubation, the disks were snap-frozen in liquid nitrogen, and the $^{14}$C label in the soluble, insoluble, and starch fractions was determined.

To assess the rate of starch synthesis from $^{14}$C data, estimates of the specific activity of the hexose phosphate were used from Carrari et al. (and Danilo Centeno, personal communication) (*11*). The experimental conditions were almost identical in both studies. Values of 0.24 ± 0.04 Bq $nmol^{-1}$ $gFWT^{-1}$ ($n$ = 4) were measured at 21, 35, and 49 DPA. We assumed that this holds true for the stages of development we examined, that is, 16, 25, 35, 40, 45, and 51 DPA. Conversion of data from Bq $gDWT^{-1}$ to μmol of hexose $gDWT^{-1}$ $h^{-1}$ was done as described in ref *16*. Calculation of rates of starch accumulation at each DPA ($mgDWT^{-1}$) was done by converting mg

**Table 1.** Relative Distribution of $^{14}C$ Incorporation into Different Fractions from Freshly Excised Tomato Pericarp Disks (cv. Moneymaker)[a]

| | relative distribution of $^{14}C$ (%) in different fractions compared to total $^{14}C$ uptake in tomato disks | | | | | |
|---|---|---|---|---|---|---|
| fraction | 16 DPA | 25 DPA | 40 DPA | 45 DPA | 50 DPA | 60 DPA |
| ethanol-soluble | 34.0 ± 2.6 | 63.6 ± 3.1 | 88.5 ± 1.7 | 88.1 ± 1.3 | 92.1 ± 0.8 | 96.5 ± 0.2 |
| ethanol-insoluble | 63.0 ± 2.5 | 36.4 ± 3.1 | 11.4 ± 1.7 | 11.9 ± 1.3 | 7.9 ± 0.8 | 1.6 ± 0.1 |
| starch | 33.9 ± 0.8** | 14.7 ± 2.1** | 1.3 ± 0.1** | 1.9 ± 0.1 | 2.3 ± 0.2 | 1.6 ± 0.2 |
| $^{14}C$ recovered (as kBq) | 1.5 ± 0.1 | 0.65 ± 0.05 | 0.41 ± 0.05** | 0.45 ± 0.04** | 0.54 ± 0.06 | 1.3 ± 0.1 |

[a] Disks were cut from fruit at six different stages of development and were incubated in 10 mM glucose with [U-$^{14}C$]glucose at specific activity = 1.4 MBq mmol$^{-1}$ for 2 h. Total $^{14}C$ was calculated from $^{14}C$ measured in the ethanol-soluble and -insoluble fractions. Starch was measured in the insoluble fraction, and the proportion of the total label converted into this compound is indicated. Values are mean ± SEM ($n$ = 3 independent measurements). Values that are significantly different ($P$ < 0.05) between developmental stages are indicated by **.

of starch to μmol of hexose. The rate at 16 DPA was calculated by dividing starch content by the number of hours at that DPA. Rates at other stages were calculated from starch accumulated between time intervals.

**Statistical Testing.** Student's $t$ test was used to determine $P$ values. Results are significantly different if the $P$ value is < 0.05.

## RESULTS

**Starch Granule Degradation and Synthesis in Developing Tomato Fruit.** *Starch Granule Accumulation in Fruit*. A starting point for our work was to establish the way in which starch accumulates in the developing fruit (**Figure 2**). When expressed on an equal mass basis, starch accumulation is highest at 25 DPA, but the total starch reservoir per fruit increased to a maximum at 40 DPA and then decreased thereafter (**Figure 2C**,**D**). The capacity for starch biosynthesis during development was investigated by incubating pericarp disks in [U-$^{14}C$]glucose (**Table 1**). Of the total $^{14}C$ accumulated in tomato disks (Bq gFWT$^{-1}$), the proportion of $^{14}C$ label found in starch was 34% at 16 DPA, 14.7% at 25 DPA when net accumulation occurs, and ~2% at 40, 45, 50, and 62 DPA—the stages when starch is broken down (**Table 1**). Starch synthesis was higher in young fruit (16 and 25 DPA), but starch was synthesized at every stage examined (**Table 1**).

The extent to which degradation of starch was occurring was estimated by taking the difference between the rate of [U-$^{14}C$]-glucose incorporated into starch and the rate of starch accumulation (*17*). Because these values are approximations, for example, if turnover occurs, rates of synthesis will be underestimated, we focused on their relative changes through development, rather than on absolute numbers. From these calculations (**Figure 3**) we concluded that (i) the bidirectional flux of starch is highest at 16 DPA; (ii) the rate of starch degradation is biphasic, that is, it is highest in young fruit, falls as ripening progresses, and then increases again in mature fruit; and (iii) starch accumulates because the rate of synthesis exceeds the rate of degradation.

*Pulse-Chase Labeling of Tomato Fruit Disks*. The results so far suggest that a large portion of newly incorporated starch is degraded in young fruit (**Figure 3**). We tested this directly using a pulse-chase experiment. Tomato fruit disks were incubated in [U-$^{14}C$]glucose for a brief period (pulse), the pulse was removed, and the fruit was then incubated in unlabeled glucose, which should allow for further synthesis of starch (chase). If there is minimal degradation, the percentage of $^{14}C$ label in starch from the pulse should remain largely unchanged in the chase. If synthesis and degradation of starch occur at the same site, then label in starch would decrease over the chase period. The experiment was done with fruit at stages of development when net starch synthesis and degradation occur (**Table 2**). After 4.5 h of chase, a significant decrease in the relative amount of label found in starch was detected only in disks from 10 DPA fruit, suggesting a rapid rate of starch degradation at this stage. After

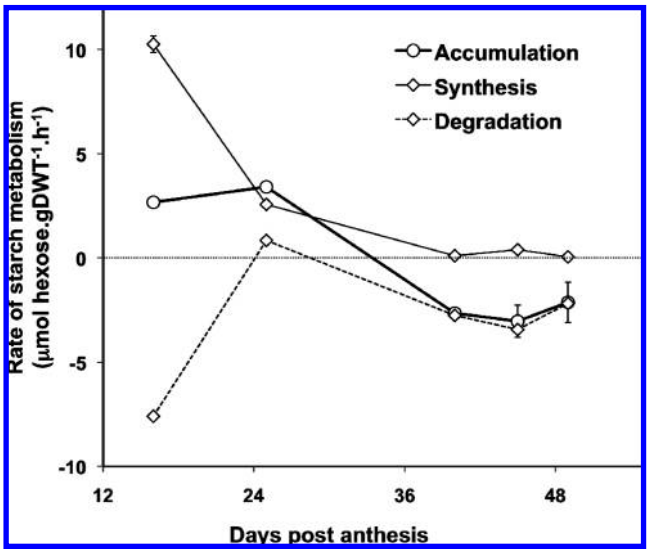


**Figure 3.** Estimates of starch synthesis and degradation in developing tomato fruit. $^{14}C$ flux data were used to calculate the rate of starch synthesis, and starch content was used to calculate starch accumulation. The rate of starch synthesis was calculated using published data of the specific activity of the hexose phosphate pool (*11*). The rate of starch degradation was obtained by subtracting the rate of synthesis from the rate of accumulation. Values are mean ± SE ($n$ = 3−6 independent measurements).

8.5 h of chase, less $^{14}C$ was measured in most samples. The relative losses of $^{14}C$ from starch compared to the amount present in starch after the 30 min pulse were 73 ± 4.4% at 10 DPA and 47 ± 2.2 and 31 ± 2.2% at 25 and 35 DPA, respectively. There was no apparent decrease of $^{14}C$ label in starch at 45 DPA during the chase in this experiment ($P$ < 0.05). At 10, 25, and 35 DPA, almost identical proportions of label were found in the 4.5 and 8.5 h chases, about 20 and 13%, respectively, compared with the amount initially present in starch after the pulse.

It is possible that the prolonged chase caused changes in fruit disk metabolism that resulted in significant starch degradation. We therefore checked that fruit disks still had the capacity to synthesize starch in the chase. Disks from fruit at 35 and 10 DPA were incubated with [U-$^{14}C$]glucose for 4 and 8.5 h, respectively. There were 79.7 ± 9.0% ($n$ = 3) and 135 ± 13% ($n$ = 3) increases in label compared to that in the pulse, respectively (data not shown). The reduced $^{14}C$ in starch in the chase is likely due to turnover and was not from senescence.

**Morphological Features of Tomato Starch Undergoing Degradation.** *Analysis of Starch Granule Size and Morphology during Development*. An important goal of this work was to observe starch granule morphology during degradation. Such analysis

**Table 2.** Pulse-Chase Experiment Assessing Starch Turnover in Developing Tomato Fruit Tissues[a]

| | $^{14}$C measured in starch expressed as % of the total $^{14}$C recovered at the end of the pulse | | | |
|---|---|---|---|---|
| | 10 DPA | 25 DPA | 35 DPA | 45 DPA |
| pulse (30 min)[b] | 50.6 ± 2.6 | 23.9 ± 1.7 | 20.6 ± 1.0 | 6.5 ± 1.5 |
| chase 1 (4.5 h) | 21.2 ± 0.6 ** | 19.2 ± 1.2 NS | 20.5 ± 1.1 NS | 4.6 ± 0.7 NS |
| chase 2 (8.5 h) | 13.7 ± 0.8 ** | 12.7 ± 0.6 ** | 14.2 ± 1.0 * | 4.4 ± 0.8 NS |

[a] Pericarp disks were incubated with [U-$^{14}$C]glucose at specific activity = 2.8 MBq mmol$^{-1}$ for 30 min. The [U-$^{14}$C]glucose was removed and the disks incubated for 4.5 h and then 8.5 h in 10 mM glucose only. The $^{14}$C measured in starch was expressed as a percentage of the total radioactivity (ethanol-soluble plus -insoluble fraction) measured in fruit disks (Bq gFWT$^{-1}$) from the pulse. Values are mean ± SE ($n$ = 4 independent measurements). Statistical significance of the difference in label found in chase 2 compared to label in pulse: **, $P < 0.01$; *, $P < 0.05$; NS, $P > 0.05$. [b] The percentage of starch incorporated during the pulse should not be compared to values in **Table 1** because of different experimental parameters.

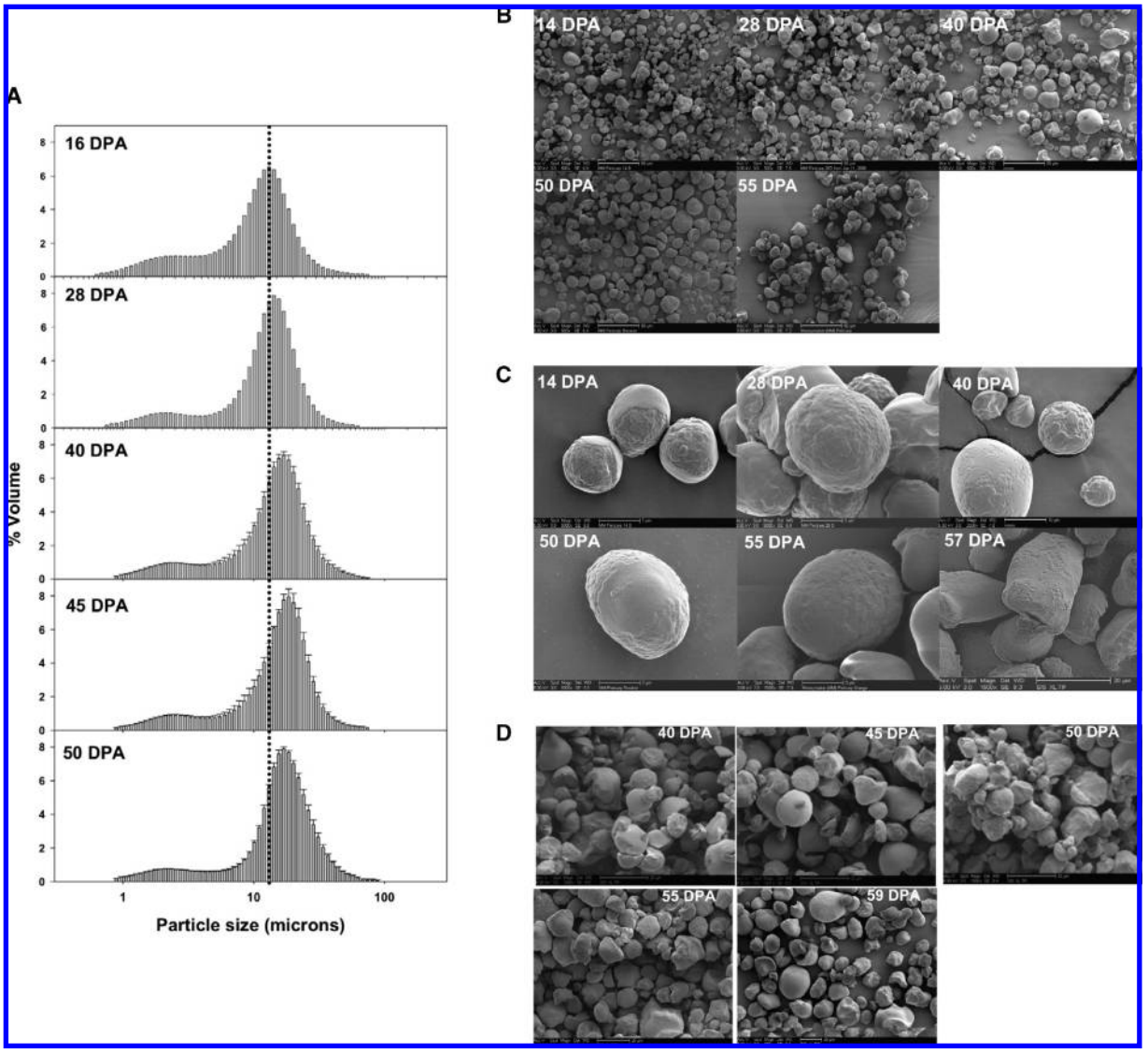


**Figure 4.** Analysis of granules from developing tomato fruit: (**A**) Particle size distribution of purified starch from ripening fruit by laser diffraction. Each graph depicts the mean ± SE of three biological replicates, except 16 and 28 DPA, which are from two replicates. Dashed lines serve as references of the modal peak at 16 DPA. The modal peak at 45 DPA appears to be larger than that at 50 DPA; however, there was no significant difference between these samples among granules of 15−20 $\mu$m, probably due to the variability in the data at 50 DPA. (**B**−**D**) Scanning electron micrographs of purified starch granules from ripening tomato fruit. Please note differences in scale bars in **C**. 40 DPA = 2500× (10 $\mu$m), 57 DPA = 1500× (20 $\mu$m), and the rest = 5000× (5 $\mu$m).

may provide clues as to how the granule is metabolized. The size distribution of the granule population in developing fruit was estimated by laser diffraction (**Figure 4A**). The pitfalls associated with the method are known, but it provides a description of a large number of granules not possible to achieve manually (*18*). Assuming that there was no selective loss of granules, the data showed that the modal granule size increased from 16 to 40 DPA but was largely unchanged from 40 to 50 DPA. Size distribution differed in older fruit, however. The proportion of small granules (< 10 $\mu$m) within the granule population decreased from 29.07 to 20.9%, whereas there was a concomitant higher proportion of larger granules from 40 to 50 DPA.

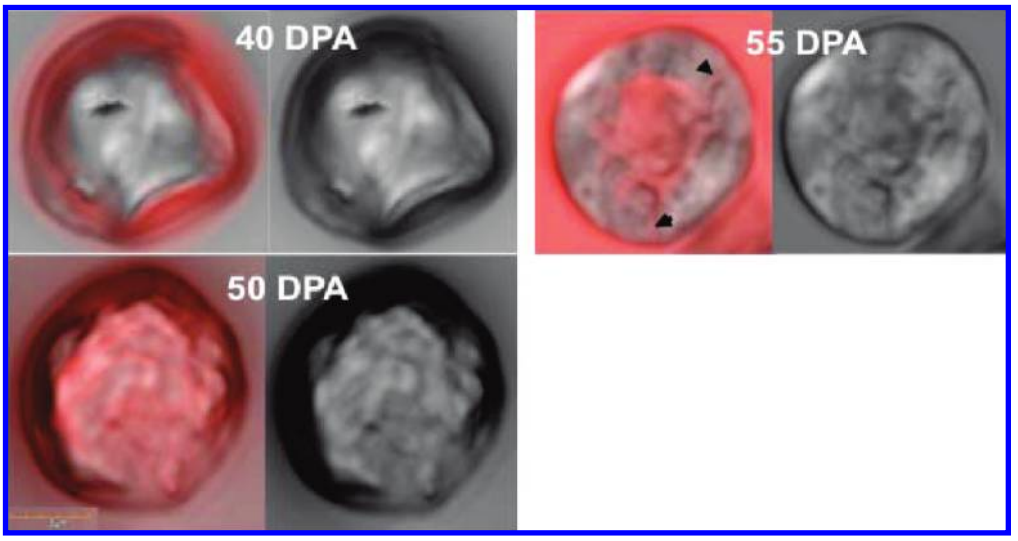


**Figure 5.** Confocal laser scanning microscopy, showing sections of fluorescent-labeled starch. Starch was purified from the same samples used for starch content, SEM, and particle size analysis. Granules were incubated with Nile Red and viewed with an objective of 60× magnification. Starch from three fruit developmental stages is shown. Arrows show channels from granule surface to interior.

The size and morphology of the granules were then examined by scanning electron microscopy (SEM). At low magnification (500×), the difference in size between granules from fruit at 14 DPA and other stages was apparent (**Figure 4B**). At higher magnification (5000×) all granules showed signs of extensive surface damage−peeling and pitting characteristic of surface degradation, that is, centripetal digestion(*19*), whereas the exterior shell of the granules was largely intact (**Figure 4C**). Granules isolated from fruit in which there was net starch degradation (40−59 DPA) were examined in greater detail (**Figure 4D**). Several granules were broken and seemed to be "half" of a whole granule with a slight hollowing of the center. The broken granules could be the result of the purification process, but the frequency with which they appeared increased at the later stages of development and may be related to the structural changes that occur in vivo.

*Confocal Laser Scanning Microscopy (CLSM) of Starch from Developing Fruit*. The large granule size and low starch content in mature fruit (**Figures 2B** and **4A**) could be explained in part if the starch granules are digested internally. To determine if starch is hydrolyzed internally in mature fruit, we used CLSM of fluorescent-stained granules, which permits visualization of space inside particles (*15*). Granules are first incubated with a fluorescent dye−carrier molecule complex. If there is free space within the granule, it would be displaced by the dye and fluoresce when viewed by CLSM. In all samples examined several granules had solid, fully intact, cores. However, as the fruit matured, granules with an internal cavity were found (**Figure 5**). The size of the void and the frequency of their appearance increased during fruit development (**Figure 5**). At 40 DPA we could not detect granules with internal decay. At 50 DPA granules showed evidence of internal decay. By 55 DPA, the cavities were so large that granules collapsed; channels starting at the granule edge and penetrating the core were visible at this stage (**Figure 5**).

*Starch from in Vitro Degraded Granules and Chilled Tomato Fruit*. In addition to examining granule degradation during fruit development, we also studied granules isolated from fruit stored at 4 °C postharvest and granules incubated with α-amylase. This may indicate if the examples of centrifugal digestion we found in ripening fruit occur generally in degrading tomato granules.

The starch incubated with α-amylase showed no change in granule size until after 54 h of incubation, when a significant amount starch was broken down (**Figure 6A**,**B**). Large holes were visible on these otherwise spherical starch granules (**Figure 6C**). The granule surface showed some uneven surfaces but was fairly smooth in comparison to that seen during ripening (**Figure 4**). Confocal microscopy showed that changes to granule internal morphology were characterized by the formation of a "cross-like" structure that enlarged after 54 h of digestion (**Figure 6D**), which could lead to splitting of the granule. Potato starch was included in the experiment for comparative purposes. The internal cavity in potato was more diffuse and thus was distinct from that seen in tomato starch (**Figure 6D**).

Degradation of starch also occurs when 40 DPA tomato fruit is stored at 4 °C for 2 weeks (unpublished observations). A prominent hole was visible on the surface of many granules isolated from fruit treated in this way (**Figure 7**). Most of the granules had a relatively smooth surface, although some of the exocorrosion visible in granules isolated from ripened fruit was also detected. CLSM of these starches showed that granules underwent centrifugal digestion (data not shown).

## DISCUSSION

The aim of this work was to understand starch granule metabolism in developing tomato fruit. The first question we asked was if starch turnover occurs during the period of active starch synthesis. As discussed, there is little direct evidence for starch degradation during periods of net synthesis in plant organs generally. Establishing whether or not it occurs is important because it would suggest that additional fluxes and enzymatic steps should be considered prior to metabolic engineering of carbohydrate composition in tomato fruit (*12*, *20*, *21*). We were able to detect turnover of starch in tomato fruit and showed that it is developmentally regulated.

The following points are emphasized with regard to the data. First, the rate of starch biosynthesis and degradation was maximal in very immature fruit (10−16 DPA) (**Figure 3**). The rate of starch degradation fell to zero ∼28 DPA but increased again around 40 DPA, but was never as high as in the fruit at 10−16 DPA. This is surprising because at 40 DPA and beyond there is net loss of starch (**Figures 2** and **3**). Second, no degradative flux of starch was detected from the pulse-chase experiment at 45 DPA. This contradicts the increase in degradation rate observed in **Figure 2**. The pulse-chase results could be explained if degradation at 45 DPA occurs at a different site on the granule where

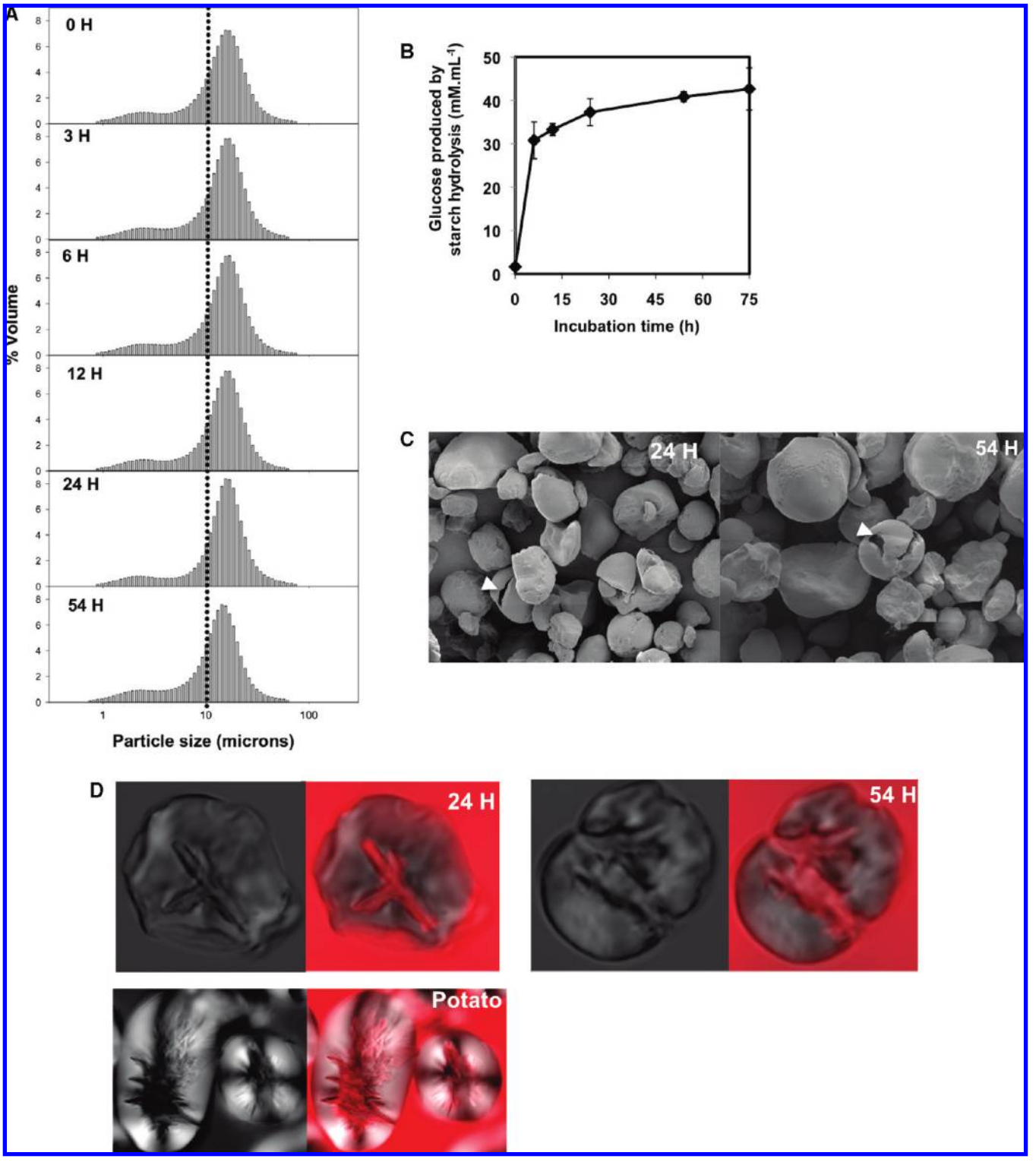


**Figure 6.** Characteristics of starch isolated from fruit at 40 DPA after in vitro digestion by α-amylase: (**A**) particle size analysis of starch after digestion with 100 U of α-amylase for the indicated length of time (sufficient granules from the 72 h incubation could not be obtained; data were derived from three biological replicates); (**B**) glucose produced from digested starch; (**C**) scanning electron micrographs of starch after 24 and 54 h of incubation with α-amylase; (**D**) confocal microscopy showing sections of fluorescent starch granules digested at 24 and 54 h (potato starch granules were digested with 1000 U of α-amylase for 24 h and were included as a control).

starch is not deposited. We hypothesized that centrifugal or inside-out digestion of starch occurs after 45 DPA. Particle size analysis (**Figures 2** and **4**) and confocal light microscopy of these starch samples together supported the idea that centrifugal digestion can occur in granules from mature fruit. This leads us to suggest that there are two phases of starch degradation with differing regiotemporal occurrences that are linked to the fruit developmental stage. In early stages, degradation may be a normal part of synthesis, whereas in older fruit, degradation is related to net loss of starch.

There are other factors that may explain our results. The increase in the proportion of larger granules seen from 40 DPA

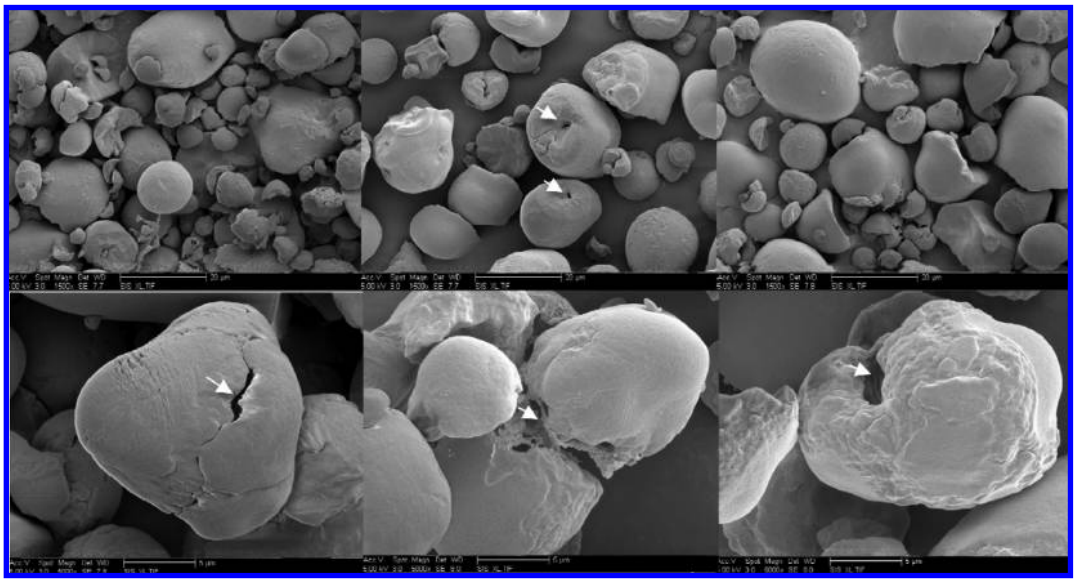

**Figure 7.** Scanning electron microscopy of starch purified from tomatoes. Fruit was stored for 2 weeks postharvest at 4 °C followed by 1 day of room temperature incubation. Arrows show openings at the granule surface that may be related to degradation by enzymatic activity.

onward may be overestimates if small granules were selectively degraded (**Figure 4A**). We assume that any loss of starch would be detected by the pulse-chase experiment, and at 45 DPA none was detected (**Table 2**). Second, our flux estimates may be criticized because disks and not whole fruit were used. However, other studies of carbohydrate metabolism show that disks yield the same results compared to whole fruit feeding (*11*). Finally, the irregularities on the granule surface may not be due to exocorrosion from turnover but could be from the morphology of the plastid. This does not change the central argument that degradation occurs in different regions of the granule in young versus older fruit. Therefore, the data presented collectively support the view of starch degradation we proposed.

The results of the pulse-chase experiment also led to two other interesting observations. First, the amount of starch synthesized in tomato fruit is dependent on the availability of substrate (*10*). The proportion of $^{14}C$ label in starch compared to total $^{14}C$ label measured decreased to 20 and 13% in disks at 10, 25, and 35 DPA during the two chase periods irrespective of the proportion found in the pulse (**Table 2**). This is best explained if the amount of starch synthesized is directly proportional to the concentration of substrate, that is, glucose in the tissue (*10*, *12*), as shown by N'tchobo et al. (*10*). Second, the pulse-chase results suggest that fruit sugar concentration and the rates of starch degradation and synthesis are highly interdependent in tomato fruit. At 10 DPA a high proportion of glucose label was partitioned to starch and there is maximal synthesis and degradation. These parameters were all reduced as the fruit aged (**Table 1** and **Figure 3**). If universally true, it poses a challenge for engineering starch metabolism in this species. It may not be easy to uncouple degradation from synthesis.

A second question we wanted to address was the manner in which tomato starch is degraded. We found that granules from fruit held in cold storage and or granules treated with α-amylase may be degraded primarily by centrifugal digestion (**Figures 4**, **6**, and **7**), lending credibility to the idea that tomato starch in developing fruit can also be broken down in this way. Differences in granule morphology were seen; for example, in developing fruit there was significantly more exocorrosion than in the other starch samples, and cold-induced degradation produced a single large hole on the granule. Tomato granules did not show the "web" of perforations characteristic of degrading starch from cereal endosperm (*22*); however, exocorrosion was more severe than that seen in potato starch (*15*). The "signature" of the attack of the starch-degrading enzymes on starch will depend on the crystalline structure of the granule. For example, after digestion with α-amylase, the architecture of the cavity inside the digested potato granule was different from that in tomato starch (**Figure 6D**).

The model we propose for tomato fruit starch degradation during ripening is best explained by a combination of models C and D (**Figure 1**). In immature fruit (10−16 DPA) there is very active turnover of starch at the site of synthesis, which decreases during development. Granules grow rapidly until ∼28 DPA because a greater proportion of sugar is diverted for starch biosynthesis and starch synthesis occurs at higher rates. From ∼40 DPA onward, there may be continued granule growth by starch deposition, although at a reduced rate, but net loss of starch occurs because of an increased rate of starch degradation. The starch degraded may be from within a larger granule and/or from the complete degradation of small granules.

In summary, the high starch metabolic activity at 10−16 DPA is consistent with the establishment of the fruit as a major sink (*23*). Bidirectionality of starch fluxes could allow the fruit to rapidly respond to sudden changes in conditions that may demand either carbon usage or storage. This may be especially critical during early growth (*12*, *24*, *25*). Ripening fruit (40 DPA and older) is characterized by higher rates of degradation and loss of starch, but a small proportion of sugar is retained for synthesis. Spatial segregation of starch degradation and synthesis at this stage would allow the granule to remain intact longer than if these processes occurred at the same site. This pattern of starch degradation may have evolved to enhance metabolic flexibility in fruit and perhaps underscores the central role starch metabolism plays in tomato fruit development.

## ACKNOWLEDGMENT

We thank Dr. Danilo Centeno for advice on $^{14}C$-feeding experiments and Michael Ngyugen and Michael Garcia for technical assistance. Belinda Martineau's assistance with editing is acknowledged, as are the very helpful comments by the reviewers and Prof. Alison Smith, which improved the manuscript.

## LITERATURE CITED


(1) Economic Research Service, U. *Commodity Highlights* **2004**, June 24, 11.

(2) Obiadalla-Ali, H. *Understanding of Carbon Partitioning in Tomato Fruit*; Max-Planck Institute of Molecular Plant Physiology: Golm, Germany, 2003.

(3) Obiadalla-Ali, H.; Fernie, A. R.; Kossmann, J.; Lloyd, J. R. Developmental analysis of carbohydrate metabolism in tomato (*Lycopersicon esculentum* cv. Micro-Tom) fruits. *Physiol. Plant*. **2004**, *120* (2), 196–204.

(4) Schaffer, A. A.; Petreikov, M. Sucrose-to-starch metabolism in tomato fruit undergoing transient starch accumulation. *Plant Physiol*. **1997**, *113* (3), 739–746.

(5) daSilva, P. M. F. R.; Eastmond, P. J.; Hill, L. M.; Smith, A. M.; Rawsthorne, S. Starch metabolism in developing embryos of oilseed rape. *Planta* **1997**, *203* (4), 480–487.

(6) Smith, A. M.; Zeeman, S. C.; Smith, S. M. Starch degradation. *Annu. Rev. Plant Biol*. **2005**, *56*, 73–98.

(7) Beckles, D. M.; Craig, J.; Smith, A. M. ADP-glucose pyrophosphorylase is located in the plastid in developing tomato fruit. *Plant Physiol*. **2001**, *126* (1), 261–266.

(8) Robinson, N. L.; Hewitt, J. D.; Bennett, A. B. Sink metabolism in tomato fruit.1. Developmental-changes in carbohydrate metabolizing enzymes. *Plant Physiol*. **1988**, *87* (3), 727–730.

(9) Beckles, D. M. *The Subcellular Location of ADPglucose Pyrophosphorylase in Starch-Storing Cells*; University of Cambridge: Cambridge, U.K., 1998.

(10) N'tchobo, H.; Dali, N.; Nguyen-Quoc, B.; Foyer, C. H.; Yelle, S. Starch synthesis in tomato remains constant throughout fruit development and is dependent on sucrose supply and sucrose synthase activity. *J. Exp. Bot*. **1999**, *50* (338), 1457–1463.

(11) Carrari, F.; Baxter, C.; Usadel, B.; Urbanczyk-Wochniak, E.; Zanor, M. I.; Nunes-Nesi, A.; Nikiforova, V.; Centero, D.; Ratzka, A.; Pauly, M.; Sweetlove, L. J.; Fernie, A. R. Integrated analysis of metabolite and transcript levels reveals the metabolic shifts that underlie tomato fruit development and highlight regulatory aspects of metabolic network behavior. *Plant Physiol*. **2006**, *142* (4), 1380–1396.

(12) Nguyen-Quoc, B.; Foyer, C. H. A role for 'futile cycles' involving invertase and sucrose synthase in sucrose metabolism of tomato fruit. *J. Exp. Bot* **2001**, *52* (358), 881–889.

(13) Luengwilai, K.; Beckles, D. M. Structural Investigations and morphology of tomato fruit starch. *J. Agric. Food Chem*. **2009**, *57*, 282–291.

(14) Huber, K. C.; BeMiller, J. N. Visualization of channels and cavities of corn and sorghum starch granules. *Cereal Chem*. **1997**, *74* (5), 537–541.

(15) Apinan, S.; Yujiro, I.; Hidefumi, Y.; Takeshi, F.; Myllarinen, P.; Forssell, P.; Poutanen, K. Visual observation of hydrolyzed potato starch granules by alpha-amylase with confocal laser scanning microscopy. *Starch−Staerke* **2007**, *59* (11), 543–548.

(16) Alonso, A. P.; Vigeolas, H.; Raymond, P.; Rolin, D.; Dieuaide-Noubhani, M. A new substrate cycle in plants. evidence for a high glucose-phosphate-to-glucose turnover from in vivo steady-state and pulse-labeling experiments with [C-13]glucose and [C-14]glucose. *Plant Physiol*. **2005**, *138* (4), 2220–2232.

(17) Geigenberger, P.; Stitt, M. A futile cycle of sucrose synthesis and degradation is involved in regulating partitioning between sucrose, starch and respiration in cotyledons of germinating *Ricinus communis* L seedlings when phloem transport is inhibited. *Planta* **1991**, *185* (1), 81–90.

(18) Wilson, J. D.; Bechtel, D. B.; Todd, T. C.; Seib, P. A. Measurement of wheat starch granule size distribution using image analysis and laser diffraction technology. *Cereal Chem*. **2006**, *83* (3), 259–268.

(19) Puncha-Arnon, S.; Puttanlek, C.; Rungsardthong, V.; Pathipanawat, W.; Uttapap, D. Changes in physicochemical properties and morphology of canna starches during rhizomal development. *Carbohydr. Polym*. **2007**, *70* (2), 206–217.

(20) Hargreaves, J. A.; Aprees, T. Turnover of starch and sucrose in roots of *Pisum sativum*. *Phytochemistry* **1988**, *27* (6), 1627–1629.

(21) Hill, S. A.; Aprees, T. Fluxes of carbohydrate-metabolism in ripening bananas. *Planta* **1994**, *192* (1), 52–60.

(22) Fannon, J. E.; Hauber, R. J.; Bemiller, J. N. Surface pores of starch granules. *Cereal Chem*. **1992**, *69* (3), 284–288.

(23) Wang, F.; Sanz, A.; Brenner, M. L.; Smith, A. Sucrose synthase, starch accumulation, and tomato fruit sink strength. *Plant Physiol*. **1993**, *101* (1), 321–327.

(24) Alonso, A. P.; Raymond, P.; Rolin, D.; Dieuaide-Noubhani, M. Substrate cycles in the central metabolism of maize root tips under hypoxia. *Phytochemistry* **2007**, *68* (16−18), 2222–2231.

(25) Schwender, J.; Ohlrogge, J.; Shachar-Hill, Y. Understanding flux in plant metabolic networks. *Curr. Opin. Plant Biol*. **2004**, *7* (3), 309–317.


**Received May 13, 2009. Revised manuscript received August 7, 2009. Accepted August 10, 2009. The Anandamahidol Foundation supported K.L. This work was funded by National Science Foundation Grant MCB-0620001 to D.M.B. and University of California Experimental Station Hatch Act Fund CA-D*-PLS-7821-H.**